JPET Fast Forward. Published on November 8, 2018 as DOI: 10.1124/jpet.118.253674
This article has not been copyedited and formatted. The final version may differ from this version.

Title Page

A fentanyl vaccine alters fentanyl distribution and protects against fentanyl-induced effects in mice and rats

Raleigh MD, Baruffaldi F, Peterson SJ, Le Naour M, Harmon TM, Vigliaturo JR, Pentel PR, and Pravetoni M

Hennepin Healthcare Research Institute (formerly Minneapolis Medical Research Foundation, MDR, BF, SJP, TMH, JRV, PRP, MP), University of Minnesota College of Pharmacy Department of Medicinal Chemistry (MLN), MLN BioPharma Consulting LLC (MLN), University of Minnesota Medical School Departments of Pharmacology (MP), Medicine (PRP and MP), and Center for Immunology (MP)

Running Title Page

Vaccine protects against fentanyl-induced respiratory depression

Corresponding author:

Michael Raleigh

Hennepin Healthcare Research Institute

701 Park Ave, Suite #S3.340

Minneapolis, MN 55415

612-873-6855

rale0011@umn.edu

Number of text pages: 37

Number of tables: 0

Number of figures: 5

Number of references: 47

Number of words in the *Abstract:* 207

Number of words in the *Introduction:* 825

Number of words in the *Discussion:* 1,263

Abbreviations: arterial oxygen saturation (SaO_2), bovine serum albumin (BSA), enzyme-linked immunosorbent assay (ELISA), keyhole limpet hemocyanin (KLH), opioid use disorder (OUD), ovalbumin (OVA), percent maximum possible effect (%MPE)

Recommended section assignment: Drug Discovery and Translational Medicine

Abstract

Fentanyl is an extremely potent synthetic opioid that has been increasingly used to adulterate heroin, cocaine and counterfeit prescription pills leading to an increase in opioid-induced fatal overdoses in the US, Canada, and Europe. A vaccine targeting fentanyl could offer protection against toxic effects of fentanyl in both recreational drug users and others in professions at risk of accidental exposure. This study focuses on the development of a vaccine consisting of a fentanyl hapten (F) conjugated to keyhole limpet hemocyanin (KLH) carrier protein or to GMP-grade subunit KLH (sKLH). Immunization with F-KLH in mice and rats reduced fentanyl-induced hotplate antinociception and in rats reduced fentanyl distribution to brain compared to controls. F-KLH did not reduce antinociceptive effects of equianalgesic doses of heroin or oxycodone in rats. To assess vaccine effect on fentanyl toxicity, rats immunized with F-sKLH or unconjugated sKLH were exposed to increasing s.c. doses of fentanyl. Vaccination with F-sKLH shifted the dose-response curves to the right for both fentanyl-induced antinociception and respiratory depression. Naloxone reversed fentanyl effects in both groups, showing that its ability to reverse respiratory depression was preserved. These data demonstrate pre-clinical selectivity and efficacy of a fentanyl vaccine and suggest that vaccines may offer a therapeutic option in reducing fentanyl-induced side effects.

Introduction

Opioid use disorders (OUD) and the fatal overdose epidemic have been a growing public health burden with over 33,000 opioid-related deaths in 2015 in the US alone (Rudd et al., 2016). The incidence of fatal overdoses from synthetic opioids increased 100% from 2015 to 2016, largely driven by illicitly-manufactured fentanyl (Rudd et al., 2016; Seth et al., 2018). Fentanyl and its analogs have been involved in more than 50% of opioid-related fatalities in the US (O'Donnell et al., 2017). Fentanyl (Fig. 1A) is a schedule II opioid agonist with an extremely high *in vivo* potency of 100-200 times than that of morphine and has been increasingly used as an adulterant in heroin and counterfeit prescription opioids because of its potency, ease of chemical feasibility, and low manufacturing costs (Schneider and Brune, 1986; Molina-Martinez et al., 2014; DEA, 2016b; Frank and Pollack, 2017). Overdose deaths from heroin or hydrocodone/acetaminophen laced with fentanyl or its derivatives carfentanil, acetylfentanil, and alfentanil have been increasingly reported in North America (Armenian et al., 2018). The presence of fentanyl was also recorded in fatal overdoses related to cocaine, benzodiazepines, antidepressants, and other counterfeit or illicit drugs (Jones et al., 2018). In addition to fentanyl misuse in patients with OUD, fentanyl and its derivatives have also been used as chemical agents for incapacitation in military scenarios (Riches et al., 2012). Finally, fentanyl and its analogs pose a potential risk for law enforcement officials, first responders, airport or custom personnel and their canine units (DEA, 2016a). These data suggest that development of novel treatment modalities to reduce the incidence or severity of accidental overdoses from fentanyl and its derivatives could have substantial public health impact.

The current treatment for fentanyl overdose is naloxone, an opioid antagonist. Distribution of naloxone to high-risk populations is being expanded in the US and has been shown to be a cost-effective strategy for decreasing overdose deaths in both the US and UK (Wheeler et al., 2015;

Langham et al., 2018). However, for naloxone to be effective administration is required shortly after exposure and with proper technique. Due to this consideration, as well as fentanyl's potency, naloxone may not always be sufficient to rapidly reverse fentanyl-induced respiratory depression (Clarke et al., 2005; Tomassoni et al., 2017). Also, administration of naloxone may precipitate opioid-withdrawal syndrome and cause severe side effects (Evans et al., 1973; Clarke et al., 2005; Rzasa Lynn and Galinkin, 2018). Prophylactic vaccination against fentanyl could be a cost-effective, long-lasting intervention to reduce the incidence or severity of fentanyl overdose.

Opioid vaccines have been explored pre-clinically as a treatment for OUD and have been effective in rodent and non-human primate models (Stowe et al., 2011; Bremer and Janda, 2012; Pravetoni et al., 2012b; Matyas et al., 2013; Raleigh et al., 2013; Schlosburg et al., 2013; Bremer et al., 2014; Raleigh et al., 2014; Bremer et al., 2017; Raleigh et al., 2017). Opioid vaccines elicit opioid-specific antibodies that bind to the targeted opioids in the blood and reduce their distribution to the brain, reducing their behavioral and toxic effects. Vaccine efficacy is greatest when the levels of antibody produced are high and the opioid dose is low. Because fentanyl is quite potent and has a relatively low toxic dose compared to other abused opioid such as heroin or oxycodone, it is a particularly attractive candidate for this approach.

A limited number of studies showed pre-clinical proof of concept for immunotherapy against fentanyl and its analogs in mice, rabbits, and dogs (Torten et al., 1975; Bremer et al., 2016; Hwang et al., 2018). These studies showed that fentanyl-specific antibodies reduced hotplate antinociception and fentanyl-induced respiratory depression following small fentanyl doses (Torten et al., 1975; Bremer et al., 2016; Hwang et al., 2018). These studies involved either passive immunization with polyclonal antibodies or active vaccination using Freund's complete adjuvant intradermally (Henderson et al., 1975; Torten et al., 1975) or other adjuvants administered i.p. (Bremer et al., 2016; Hwang et al., 2018), which may not be feasible in humans.

The aim of this study was to determine the efficacy of a fentanyl vaccine adsorbed on alum adjuvant and administered i.m. in mice and rats. The F-KLH vaccine was developed using a fentanyl-based hapten (F) conjugated to either the native decamer keyhole limpet hemocyanin (KLH) carrier protein or the GMP-grade subunit KLH (sKLH) by means of a tetraglycine linker using carbodiimide chemistry. This vaccine design is analogous to other opioid vaccines that are being prepared for clinical use (Raleigh et al., 2017; Raleigh et al., 2018). Mice and rats immunized with F-KLH had lower fentanyl-induced antinociception compared to controls. Rats immunized with F-KLH had lower brain fentanyl concentrations following an i.v. dose of fentanyl compared to controls. In a separate cohort of rats, F-sKLH reduced fentanyl-induced hotplate antinociception, respiratory depression, and bradycardia over a range of cumulative s.c. fentanyl doses. Together, these data suggest that a fentanyl vaccine could be a viable option for reducing the respiratory depressive effects of fentanyl in humans.

Materials and methods

Ethics statement

These studies were carried out in strict accordance with the recommendations in the Guide for the Care and Use of Laboratory Animals of the National Institutes of Health. Animal protocols were approved by the Hennepin Healthcare Research Institute Animal Care and Use Committee. Surgery was performed under ketamine (75 mg/kg) and dexmedetomidine (0.05 mg/kg) anesthesia, animals were euthanized by CO_2 inhalation using AAALAC approved chambers, and all efforts were made to minimize suffering.

Overview of the fentanyl hapten synthesis

The F hapten (Scheme 1, **[8])** was synthesized as depicted in **scheme 1**. Briefly, piperidone monohydrate hydrochloride (Scheme 1, **[1])** propanamide was alkylated with 2-(Bocamino)ethylbromide in the presence of potassium carbonate in acetonitrile to provide the *N*-substituted piperidine intermediate (Scheme 1, **[2])** with good yield. Reductive amination with aniline of (Scheme 1, **[2])** mediated by sodium cyanoborohydride in the presence of an equimolar amount of acetic acid yielded the 4-piperidineamine precursor (Scheme 1, **[3])** in excellent yield (91%). Then, **[3]** was acylated using propionyl chloride in the presence of Hunig's base (DIPEA) to provide compound (Scheme 1, **[4]).** Acid-mediated *N*-Boc terminal group deprotection followed by acylation with glutaric anhydride in presence of pyridine led to carboxylic acid (Scheme 1, **[6]).** Both steps did not require any further purification. The linker $(Gly)_4$-OtBu (Pravetoni et al., 2012a) was attached in classic fashion using HBTU and Hunig's base as coupling agents. Lastly, the tert-butyl ester **[7]** was hydrolyzed using 20% of trifluoracetic acid in dichloromethane to afford hapten **[8]**.

Fentanyl hapten

All commercial reagents and anhydrous solvents were used without further purification or distillation. Analytical thin-layer chromatography (TLC) was performed on EM Science silica gel 60 F254 (0.25 mm). Plates were visualized by UV light, iodine vapor, or ninhydrin solution. Flash column chromatography was performed on Thermo Fisher Scientific silica gel (230 – 400 mesh) unless otherwise noted. Nuclear magnetic resonance (1H NMR (400 MHz), 13C NMR (100 MHz)) spectra were determined on a Bruker 400 instrument unless otherwise noted. Chemical shifts for 1H NMR are reported in parts per million (ppm) relative to chloroform (7.26 ppm) and coupling constants are in hertz (Hz). Chemical shifts are expressed in ppm and coupling constants (*J*) are in hertz (Hz). Peak multiplicities are abbreviated: broad, br; singlet, s; doublet, d; triplet, t; and multiplet, m. Chemical shifts for 13C NMR were reported in ppm relative to the center line of a triplet at 77.0 ppm for chloroform. ESI mode mass spectra were recorded on a BrukerBioTOF II mass spectrometer, and the data were consistent with the considered structures. Elemental analyses for the target compound were performed by M-H-W Laboratories, Phoenix, AZ. Analytical data confirmed the purity of the products was ≥ 95%.

tert-butyl (2-(4-oxopiperidin-1-yl)ethyl)carbamate [2]

4-piperidone monohydrate hydrochloride **[1]** 2.0 g, 13 mmol) was dissolved in acetonitrile (40 mL) in a 250 mL round-bottom flask equipped with a large stir bar and a condenser. The colorless solution was treated sequentially with potassium carbonate (K_2CO_3, 3.26 g, 23.6 mmol) and 2-(Boc-amino)ethylbromide (1.96 mL, 11.8 mmol) at ambient temperature. The resulting suspension was vigorously stirred and refluxed at 80°C for 8 h. After 8 hours, the mixture was cooled to ambient temperature, transferred to a separatory funnel and partitioned (CH_2Cl_2//H_2O). The organic phase was washed with brine, saturated $NaHCO_3$ (2X 100 mL), dried over Na_2SO_4 and concentrated *in vacuo* to give a yellow oil. The oily mixture was purified by flash column chromatography (EtOAc/hexanes: 1/1) to give [2] as a light yellow oil (2.5 g, 88%). ^{1}H NMR (400

MHz, C*D*Cl$_3$) δ 6.76 (br, 1H, NH); 3.26 (t, 2H, *J*= 7.3 Hz); 2.67-2.59 (m, 4H); 2.46 (t, 2H, *J*= 7.3 Hz); 2.22-2.16 (m, 4H); 1.42 (s, 9H); ^{13}C NMR (77 MHz, C*D*Cl$_3$) δ 207.1; 155.9; 79.6; 55.3 (2C); 53.4; 41.2 (2C); 38.9; 28.4 (3C). ESI-TOF MS calculated for $C_{12}H_{22}N_2O_3$, *m/z* 242.32, found 243.43 $[MH]^+$.

tert-butyl (2-(4-(phenylamino)piperidin-1-yl)ethyl)carbamate [3]

Aniline (750 μL, 8.2 mmol) was taken up in methylene chloride in a 100 mL round-bottom flask equipped with a stir bar. The light brown solution was placed on an ice bath and treated dropwise with acetic acid (AcOH, 460 μL, 8.2 mmol). To the mixture, *tert*-butyl (2-(4-oxopiperidin-1-yl)ethyl)carbamate **[2]** (2 g, 8.2 mmol) was added as a solution in methylene chloride, followed by the careful, slow addition of sodium cyanoborohydride ($NaBH_3CN$, 773 mg, 12.3 mmol) in small portions. The reaction mixture was stirred at 80°C for 14 h. After this time, methanol was added to the mixture, and all contents transferred to a separatory funnel. The mixture was partitioned (CH_2Cl_2//saturated $NaHCO_3$). Once neutralized, the organic phase was washed with brine, dried over Na_2SO_4 and concentrated in vacuo to give a light brown oil. The oily mixture was purified by flash column chromatography (EtOAc/hexanes: 7/3) to give **[3]** as a light yellow oil (2.25 g, 86%). ^{1}H NMR (400 MHz, C*D*Cl$_3$) δ 7.37 (d, 2H, *J*= 7.8 Hz); 7.27-7.25 (m, 3H); 6.35 (br, 1H, NH); 5.21 (br, 1H, NH); 3.84 (m, 1H); 3.77-3.58 (m, 4H); 3.21-3.14 (m, 4H); 2.31-2.26 (m, 4H); 1.43 (s, 9H); ^{13}C NMR (77 MHz, C*D*Cl$_3$) δ 156.7; 147.6; 129.5 (2C); 120.8; 113.5 (2C); 79.5; 64.3; 53.9; 52.0 (2C); 39.7; 30.3 (2C); 26.8 (3C). ESI-TOF MS calculated for $C_{18}H_{29}N_3O_2$, *m/z* 319.23, found 320.17 $[MH]^+$.

tert-butyl (2-(4-(N-phenylpropionamido)piperidin-1-yl)ethyl)carbamate [4]

Compound **[3]** (1.5 g, 4.7 mmol) was dissolved in methylene chloride in a 100 mL round bottom flask equipped with a small stir bar and was treated with diisopropylethylamine (DIPEA, 1.64 mL,

9.4 mmol). The solution was cooled with an ice bath and treated dropwise with propionyl chloride (0.81 mL, 9.4 mmol). The resulting mixture was stirred for 2h at ambient temperature. The mixture was transferred to a separatory funnel and partitioned (CH_2Cl_2//H_2O). The organic phase was washed with brine, saturated $NaHCO_3$, dried over anhydrous Na_2SO_4 and evaporated *in vacuo* to give a yellow oil that was purified by flash column chromatography (EtOAc/hexanes: 4/6) to furnish **[4]** as a light yellow oil (1.68 g, 95%). ^{1}H NMR (400 MHz, C*D*Cl$_3$) δ 7.40-7.27 (m, 3H); 7.26 (d, 2H, *J*= 7.8 Hz); 4.72 (m, 1H); 3.98 (t, 2H, J= 7.1 Hz); 3.27-3.17 (m, 4H); 2.82-2.74 (m, 4H); 2.15-2.08 (m, 4H); 1.40 (s, 9H); 1.01 (t, 3H, *J*= 7.1 Hz); ^{13}C NMR (77 MHz, C*D*Cl$_3$) δ 174.6; 155.9; 137.9; 128.3 (2C); 128.0; 127.5 (2C); 81.5; 62.5; 53.9; 53.4 (2C); 40.1; 28.2; 26.8 (3C); 25.9 (2C); 10.3. ESI-TOF MS calculated for $C_{21}H_{33}N_3O_3$, *m/z* 319.23, found 320.17 $[MH]^+$.

N-(1-(2-aminoethyl)piperidin-4-yl)-N-phenylpropionamide [5]

Trifluoroacetic acid (TFA, 20% volume) was added to a solution of compound **[4]** (1 g, 3.1 mmol) in dichloromethane (40 ml). The resultant solution was stirred at room temperature. Upon complete disappearance of starting material, the solvent was removed under vacuum. The crude reaction mixture was co-evaporated with large volumes of dichloromethane several times to yield a white solid that was placed under vacuum overnight. The resulting white solid (1.45 g, quantitative) was used without further purification. ^{1}H NMR (400 MHz, C*D*Cl$_3$) δ 12.2 (br, 1H); 7.37-7.29 (m, 3H); 7.03 (d, 2H, *J*= 7.8 Hz); 4.62 (m, 1H); 3.83 (t, 2H, J= 7.1 Hz); 3.18-3.05 (m, 4H); 2.75-2.62 (m, 4H); 2.15-2.08 (m, 4H); 0.98 (t, 3H, *J*= 7.1 Hz); ^{13}C NMR (77 MHz, C*D*Cl$_3$) δ 177.3; 161.4; 159.3; 136.2; 126.2 (2C); 126.1; 125.9 (2C); 113.2; 112.9; 85.7; 62.3; 54.2; 53.4 (2C); 41.2; 27.2; 23.9 (2C); 10.3. ESI-TOF MS calculated for $C_{20}H_{27}F_6N_3O_5$, *m/z* 503.19, found 377.25 $[MH\text{-}TFA]^+$, 276.33 $[MH\text{-}2xTFA]^+$.

5-oxo-5-((2-(4-(N-phenylpropionamido)piperidin-1-yl)ethyl)amino)pentanoic acid [6]

JPET Fast Forward. Published on November 8, 2018 as DOI: 10.1124/jpet.118.253674
This article has not been copyedited and formatted. The final version may differ from this version.

To a solution of amine **[5]** (1 g, 2 mmol) dissolved in dichloromethane with pyridine (0.64 mL, 6 mmol), glutaric anhydride (228 mg, 2 mmol) was added dropwise. The mixture was stirred at room temperature overnight. After disappearance of starting material, the solvent was concentrated to dryness; the residue was co-evaporated with toluene (3X). The mixture was transferred to a separatory funnel and partitioned (CH_2Cl_2//H_2O). The organic phase was washed with brine, saturated $NaHCO_3$, dried over anhydrous Na_2SO_4 and evaporated *in vacuo* to give **[6]** as a white solid (780 mg, quantitative). Compound **[6]** was used without further purification. ^{1}H NMR (400 MHz, C*D*Cl_3) δ 7.35-7.31 (m, 3H); 7.02 (d, 2H, *J*= 7.8 Hz); 4.79 (m, 1H); 4.02 (t, 2H, J= 7.1 Hz); 4.57-4.52 (m, 2H); 2.91-2.85 (m, 2H); 2.62-2.51 (m, 4H); 2.25-2.13 (m, 2H); 1.99-1.75 (m, 8H); 0.98 (t, 3H, *J*= 7.1 Hz); ^{13}C NMR (77 MHz, C*D*Cl_3) δ 178.4; 174.6; 172.6; 137.9; 128.9 (2C); 128.1; 127.5 (2C); 83.5; 59.1; 52.0 (2C); 39.2; 35.6; 32.3; 28.2; 27.6 (2C); 20.3; 10.2. ESI-TOF MS calculated for $C_{21}H_{31}N_3O_4$, *m/z* 389.23, found 390.21 $[MH]^+$.

tert-butyl (5-oxo-5-((2-(4-(N-phenylpropionamido)piperidin-1-yl)ethyl)amino)pentanoyl)glycylglycylglycylglycinate [7]

The carboxylic acid **[6]** (500 mg, 1.28 mmol) was dissolved in dichloromethane, followed by the subsequent addition of 2-(1*H*-benzotriazol-1-yl)-1,1,3,3-tetramethyluronium hexafluorophosphate (HBTU, 729 mg, 1.92 mmol) and the appropriate amine $(Gly)_4$-OtBu (Pravetoni et al., 2012a) (387 mg, 1.28 mmol). *N,N*-Diisopropylethylamine (DIPEA, 403 μL, 2.31 mmol) was then added to the mixture. The solution was stirred overnight at room temperature. The mixture was transferred to a separatory funnel and partitioned (CH_2Cl_2//H_2O). The organic phase was washed with brine, saturated $NaHCO_3$, dried over anhydrous Na_2SO_4 and evaporated *in vacuo*. The resulting mixture was purified by SiO_2 flash column chromatography (EtOAc/hexanes: 6/4) to provide **[7]** as a light yellow oil (637 mg, 74%). ^{1}H NMR (400 MHz, C*D*Cl_3) δ 7.41-7.39 (m, 3H); 7.08 (d, 2H, *J*= 7.9 Hz); 6.13 (br, 1H, NH); 4.62 (m, 1H); 3.71-3.65 (m, 10H); 3.30-3.26 (m, 2H); 3.00-2.98 (m, 2H);

JPET Fast Forward. Published on November 8, 2018 as DOI: 10.1124/jpet.118.253674
This article has not been copyedited and formatted. The final version may differ from this version.

2.55-2.49 (m, 2H); 2.32-2.15 (m, 6H); 1.93-1.80 (m, 6H); 1.43 (s, 9H); 0.98 (t, 3H, *J*= 7.1 Hz); ^{13}C NMR (77 MHz, C*D*Cl$_3$) δ 177.9; 174.8; 172.5; 171.0 (3C); 169.5; 137.8; 128.4 (2C); 128.2; 127.6 (2C); 83.3; 81.8; 59.1; 52.1 (2C); 42.4; 42.7; 41.0; 39.6; 35.5; 34.6; 28.7 (3C); 27.5 (2C); 22.2; 10.1. ESI-TOF MS calculated for $C_{33}H_{51}N_7O_8$, *m/z* 673.38, found 674.47 $[MH]^+$.

(5-oxo-5-((2-(4-(N-phenylpropionamido)piperidin-1-yl)ethyl)amino)pentanoyl)glycylglycylglycylglycine [8]

TFA (1 ml) was added to a solution of compound **[7]** (300 mg, 0.47 mmol) in dichloromethane (4 ml). The mixture was stirred at room temperature overnight. Upon complete disappearance of starting material, the solvent was removed under vacuum. The residue was re-dissolved in dichloromethane and evaporated again. This operation was repeated twice to afford a pale-yellow paste that was purified by SiO_2 flash column chromatography (MeOH/CH_2Cl_2: 2/98) to give **[8]** as a white solid (266 mg, 92%). ^{1}H NMR (400 MHz, C*D*Cl$_3$) δ 7.39-7.36 (m, 3H); 7.02 (d, 2H, *J*= 7.9 Hz); 4.59 (m, 1H); 3.69-3.62 (m, 10H); 3.21-3.18 (m, 2H); 2.98-2.92 (m, 2H); 2.47-2.42 (m, 2H); 2.29-2.16 (m, 6H); 1.91-1.82 (m, 6H); 0.97 (t, 3H, *J*= 7.1 Hz); ^{13}C NMR (77 MHz, C*D*Cl$_3$) δ 178.1; 174.6; 174.2; 172.6; 169.2 (3C); 137.9; 128.6 (2C); 128.4; 127.5 (2C); 83.4; 59.8; 53.3 (2C); 42.7; 42.9; 41.3; 39.7; 35.3; 34.7; 27.6 (2C); 22.5; 10.3. ESI-TOF MS calculated for $C_{29}H_{43}N_7O_8$, *m/z* 617.32, Found 618.31 $[MH]^+$. Analytical calculation for $C_{29}H_{43}N_7O_8$: C, 56.39; H, 7.02; N, 15.87. found: C, 56.34; H, 6.99; N, 15.91.

Vaccines

The F hapten (Fig. 1B) was conjugated through carbodiimide (EDAC) chemistry as previously described for other opioid-based haptens (Pravetoni et al., 2012a; Pravetoni et al., 2012b). Briefly, 5 mM of hapten was reacted with a 52 mM concentration of EDAC (Sigma Aldrich, St. Louis, MO) in 0.1 M MES buffer at pH 4.5, and stirred for 5 minutes at room temperature. Bovine serum

albumin (BSA), ovalbumin (OVA), KLH, or sKLH were then added to the reaction mixture at amounts of 2.8, 1.9, 2.8, and 2.8 mg, respectively, in a final volume of 1ml, and stirred for 3 hours at room temperature as described (Pravetoni et al., 2012a). Bioconjugation efficacy was indirectly measured by assessing the haptenation ratio of F-BSA by comparing the molecular weight of the unconjugated and conjugated BSA by MALDI-TOF. Conditions optimized for F-BSA led to a haptenation ratio of 8. Haptenation ratios were not determined for KLH because its molecular weight is too large to be measured by MALDI-TOF.

Drugs

Fentanyl, oxycodone, and heroin were obtained through the National Institute on Drug Abuse Drug Supply Program (Bethesda, MD) or Sigma-Aldrich (St. Louis, MO). Drug doses and concentrations are expressed as the weight of the base.

Brain and serum fentanyl concentration

Fentanyl concentrations were measured by gas chromatography mass spectrometry (GC/MS) using a modified procedure (Huynh et al., 2005). Briefly, trunk blood was collected and centrifuged following experimentation at 3100 x *g* for 3 min at 4 °C. Internal standard (D5-fentanyl, 50 μL of 1 μg/mL) was added to all serum and standard samples. Then, 0.15 mL 1.0M NaOH and 3.5 mL n-heptane with 3% 2-butanol was added to 0.5 mL serum samples. Samples were capped and rotated at approximately 15 RPM for 30 min on orbital shaker (Orbitron Rotator II Model 260250) and then centrifuged for 5 min at 1500 x *g*. The lower aqueous phase was frozen using a mixture of dry ice and acetone for 10 min. Solvent layer was transferred and placed on an N-Evap at 45 °C until solvent completely evaporated. Solvent reconstituted in 50 μL ethyl acetate, briefly vortexed, and then centrifuged for 5 min at 1500 x *g*. Samples were injected onto the GC/MS for analysis.

Antibody characterization

Antibody titers

Fentanyl-specific serum IgG antibody titers were measured as previously described for other hapten conjugates (Raleigh et al., 2013; Raleigh et al., 2017). Briefly, fentanyl conjugated to OVA (F-OVA) was used as the coating antigen for mouse studies and conjugated to BSA (F-BSA) for rat studies. Coating antigen was diluted in 0.05 M carbonite buffer pH 9.6, coated onto 96 well ELISA plates (Jackson ImmunoResearch Laboratories, Inc., West Grove, PA), and stored overnight at 4 °C. Plates were blocked with 1% gelatin in PBST for 1 hr and then stored overnight at 4 °C. The next day various dilutions of sera in 0.05 M PBST were added to the wells and plates incubated for 2 h at room temperature. After washing the plates, Fc-specific goat anti-rat or anti-mouse IgG coupled to horseradish peroxidase (Jackson ImmunoResearch Laboratories, Inc., West Grove, PA), were added and incubated at overnight at 4 °C. *O*-phenylenediamine (OPD) was used (SIGMA*FAST*™ tablet set, Sigma Life Sciences, St Louis, MO) as the reaction substrate. After 30 min of incubation, 2% oxalic acid was added to stop the enzymatic reaction. Plates were read at 492 nm on a BioTek PowerWave XS (BioTek Instruments Inc., Winooski, VT).

Estimated minimum antibody concentrations

The minimal fentanyl-specific antibody concentrations present in serum were estimated by assuming that the difference in serum fentanyl concentration in vaccinated and control rats represents the fentanyl retained in serum by the binding capacity contributed by antibody. This value was calculated by subtracting the mean control vaccine group serum fentanyl concentration from the individual serum fentanyl concentration from each vaccinated rat and multiplying by the molecular weight of IgG (150,000 Da) divided by two binding sites per IgG.

Stoichiometry

The total number of moles per kilogram of opioid-specific IgG in rats vaccinated with F-KLH or F-sKLH in *Experiment 2 and 4* was calculated as the product of the estimated antibody concentration in serum and the reported IgG volume of distribution (131 ml/kg) in rats (Bazin-Redureau et al., 1997; Pravetoni et al., 2012a).

Experiment 1: **Effect of F-KLH on opioid distribution and antinociception after single fentanyl challenge in mice**

Male BALB/c mice (Envigo, Madison, WI) 5-6 weeks old were housed in groups of 4 under 12/12-hour standard light/dark cycle. Groups of 8 mice were immunized s.c. with F-KLH or control KLH vaccine containing 25 µg immunogen and 0.5 mg aluminum hydroxide (Alhydrogel, Invitrogen, San Diego, CA). Vaccine was administered s.c. on day 0, 14, and 28. On day 35, blood was collected via submandibular bleeding for antibody characterization. On day 42 baseline antinociception was assessed by placing mice on a 54ºC hotplate and measuring the latency to respond, defined as the time until a response of hindpaw lick or jumping (Pravetoni et al., 2012a). Testing was terminated at 60 sec to avoid tissue damage. Mice received a 0.05 mg/kg s.c. dose of fentanyl. This dose was chosen because it elicited submaximal latency to respond on the hotplate in a pilot study. 30 min after dosing, mice were placed on the hotplate again to measure latency to respond. Percent maximum possible effect (%MPE) was calculated as the post-test latency minus the pre-test latency divided by the maximum time (60 sec) minus the pre-test latency times 100. Immediately after hotplate testing mice were anesthetized with isoflurane and blood and brain collected to assess drug levels.

Experiment 2: **Efficacy and selectivity of F-KLH on opioid distribution and antinociception in rats challenged with fentanyl, heroin, and oxycodone**

Male Holtzman rats (Envigo, Madison, WI) weighing 200-225 g were double housed with 12/12-hour standard light/dark cycle. Groups of 12 rats were immunized s.c. with F-KLH or control KLH

vaccine containing 25 µg immunogen and 0.5 mg aluminum hydroxide. Vaccine was administered i.m. on day 0, 21, and 42. On day 49, blood was collected via tailvein for antibody characterization. Hotplate testing was identical to *Experiment 1*, except that rats received 0.035 mg/kg s.c. dose of fentanyl. This dose was chosen because it elicited submaximal latency to respond on the hotplate in a pilot study. On day 51, KLH and F-KLH immunized rats were split into two groups and half (n=6 for KLH and n=6 for F-KLH treated rats) received 1 mg/kg heroin s.c. and the other half (n=6 for KLH and n=6 for F-KLH treated rats) received 2.25 mg/kg oxycodone s.c. and tested on the hotplate as in *Experiment 1*. These doses were chosen because they produce significant antinociception and have previously been use to test heroin and oxycodone vaccine efficacy in rats (Pravetoni et al., 2012a; Pravetoni et al., 2013; Raleigh et al., 2013). On day 58, rats were given a 0.05 mg/kg i.v. infusion of fentanyl for 1 min and blood and brain were collected 4 min later. The i.v. route was chosen, in contrast to the s.c. route commonly used for antinociception, because it provides the most rigorous challenge with regard to route, and because it corresponds to how it is most commonly encountered as an adulterant. The dose was chosen because it was a large fentanyl dose capable of testing vaccine efficacy and because fentanyl levels in serum and brain in rats at this i.v. dose was already well described (Hug and Murphy, 1981).

Experiment 3: **Fentanyl-induced antinociception and respiratory depression after repeated fentanyl challenges in rats**

Sprague Dawley rats were used in *Experiment 3* and *4* because Holtzman rats became temporarily unavailable. Male Sprague Dawley rats (Envigo, Madison, WI) weighing 200-225 g were double housed with 12/12-hour standard light/dark cycle. To determine a fentanyl dose range that produced a wide range of antinociception and respiratory depression, 8 rats were tested on the hotplate and oximeter following successive fentanyl s.c. doses. Baseline antinociception (prior to fentanyl administration) was assessed. Immediately following the hotplate test rats were placed in a 12” x 12” enclosed chamber to prevent and a MouseOx (STARR Life

Sciences Corp., Oakmont, PA) arterial oxygen saturation (SaO_2) monitor was placed via neck collar for at least 1 minute to ensure stable readings were obtained and baseline SaO_2 was measured as described (Raleigh et al., 2017). SaO_2, breath rate, and heart rates were recorded as the mean of the last 10 seconds, which correspond to 10 measurements. Rats then received fentanyl every 17 minutes s.c. so that their cumulative fentanyl dose at successive intervals was 12.5, 25, 50, and 100 μg/kg. Fifteen minutes after each fentanyl dose, antinociception and SaO_2 were again measured; this accounted for 2 minutes, resulting in the 17 minutes fentanyl dosing interval. Heart rate was obtained from the oximeter. Rats received 0.1 mg/kg naloxone s.c. immediately after the final antinociception and SaO_2 measures were obtained. The naloxone dose was chosen based on previous data (Raleigh et al., 2017) and is comparable to the maximum recommended dose (Wong, 2012). Antinociception and cutaneous SaO_2 were again measured 15 min after naloxone administration. Rats were awake throughout hotplate and oximeter testing.

Experiment 4: **Efficacy of F-sKLH on opioid distribution, antinociception, and respiratory depressive effects after repeated fentanyl challenges in rats**

Male Sprague Dawley rats (Envigo, Madison, WI) weighing 200-225 g were double housed with 12/12-hour standard light/dark cycle. Groups of 8 rats were immunized i.m. with F-sKLH or control sKLH vaccine containing 25 μg immunogen and 0.5 mg aluminum hydroxide on days 0, 21, 42, and 63. On day 70, blood was collected via tailvein for antibody characterization. On day 77, rats were tested on the hotplate and oximeter using the same protocol as in *Experiment 3*. Blood and brain were collected at the end of the experiment to measure fentanyl concentrations in these tissues.

Statistical analysis

Fentanyl-specific serum antibody titers, opioid levels, and hotplate antinociception for *Experiments 1* and *2* were compared between groups using unpaired t tests with Welsh's

correction. For *Experiment 3*, latency to respond in the hotplate nociception test and SaO_2 were compared using a repeated measures one-way ANOVA using Dunnett's multiple comparison test. For *Experiment 4*, latency to respond in the hotplate nociception test and SaO_2 were compared between groups over time by 2-way ANOVA using Sidak's multiple comparisons test while within group comparisons were done using Dunnett's multiple comparison test. Effective dose of fentanyl that caused 50% maximal effect (ED_{50}) on the antinociceptive hotplate test was performed using nonlinear regression analysis using the model *[Agonist] vs. response – Variable slope (four parameters)* with the ceiling parameter set as a constant equal to 60 seconds (maximal latency to respond). ED_{50} for % SaO_2 and breath rate could not be measured because minimum and maximum values could not be established. All statistics were performed using Prism (version 8.0a.91; GraphPad, San Diego, CA).

Results

Experiment 1: Efficacy of F-KLH on opioid distribution and antinociception after single s.c. injection of fentanyl in mice

Mice vaccinated with F-KLH had 92 ± 62 x 10^3 (mean ± SD) fentanyl-specific antibody titers. Estimated minimum antibody concentrations were 5.3 ± 1.5 μg/mL. Because of the manner in which this minimum concentration was estimated (from the concentration of fentanyl retained in serum by antibody), actual antibody concentration may have been higher. F-KLH vaccination significantly reduced fentanyl-induced antinociceptive effects on the hotplate by 60% compared to controls (Fig. 2A, $p < 0.01$). Serum fentanyl concentrations were significantly increased in F-KLH vaccinated mice compared to controls (Fig. 2B, $p < 0.001$).

Experiment 2: Efficacy of F-KLH on opioid distribution and antinociception after single s.c. injection of fentanyl in rats

Rats vaccinated with F-KLH had 9.0 ± 4.4 x 10^3 fentanyl-specific antibody titers. Estimated minimum antibody concentrations were 18.6 ± 8.5 μg/mL. The molar ratio of the fentanyl dose (0.035 mg/kg) to the estimated antibody binding sites in F-KLH vaccinated rats was 3.2. F-KLH vaccination significantly reduced fentanyl-induced antinociceptive effects on the hotplate by 93% compared to controls (Fig. 3A, $p < 0.05$). F-KLH vaccination had no effect on heroin- or oxycodone-induced antinociception (Fig. 3B and 3C, $p = 0.64$ and 0.76, respectively). One week after antinociceptive testing, rats received a 1-min infusion of 0.05 mg/kg i.v. fentanyl. The molar ratio of the fentanyl dose (0.05 mg/kg) to the estimated antibody binding sites in F-KLH vaccinated rats was 4.6. Serum fentanyl concentrations were significantly increased (Fig. 3D, $p < 0.001$) and brain fentanyl concentrations were decreased by 30% (Fig. 3E, $p < 0.05$) compared to controls.

Experiment 3: **Fentanyl-induced antinociception and respiratory depression after cumulative s.c. fentanyl dosing in rats**

Latency to respond on the hotplate was significantly increased following the 25, 50, and 100 μg/kg cumulative doses (Fig. 4A, $p < 0.001$ at all three doses) compared to baseline latencies. Naloxone returned latencies to respond on the hotplate back to baseline levels. Percent SaO_2 levels were significantly reduced following the 50 and 100 μg/kg cumulative doses (Fig. 4B, $p < 0.01$ and $p < 0.001$, respectively). Naloxone reversed % SaO_2 levels to baseline values. Heart rate (BPM) was significantly lowered following the 25, 50, and 100 μg/kg cumulative doses (Fig. 4C, $p < 0.01$ at all three doses). Naloxone treatment did not reverse BPM back to baseline ($p < 0.001$).

Experiment 4: **Efficacy of F-sKLH on opioid distribution, antinociception, and respiratory depressive effects after cumulative s.c. fentanyl dosing in rats**

Rats vaccinated with F-sKLH had 25 ± 9.6 x 10^3 fentanyl-specific antibody titers. Estimated minimum antibody concentrations were 68.2 ± 46 μg/mL. The molar ratio of the fentanyl dose (0.1 mg/kg) to the estimated antibody binding sites in F-sKLH vaccinated rats was 2.5. F-sKLH attenuated fentanyl-induced antinociception by shifting the latency to respond dose-response curve to the right on the hotplate after increasing cumulative doses of fentanyl (Fig. 4D, vaccination, $F(1,14) = 42.0$, $p < 0.001$; interaction, $F(5,70) = 10.4$, $p < 0.001$; fentanyl dose, $F(3.35,46.9) = 40.9$, $p < 0.001$). Fentanyl significantly increased latency to respond following 25 μg/kg in sKLH vaccinated rats, but only after 100 μg/kg in the F-sKLH group, compared to their baseline values. These values represent an ED_{50} of 0.02 ± 0.01 μg/kg in the sKLH group and 0.08 ± 0.06 μg/kg in the F-sKLH group, decreasing fentanyl potency by a 5.4-fold shift in the presence of fentanyl-specific antibodies. Naloxone completely reversed fentanyl-induced antinociception in both groups. F-sKLH significantly reduced fentanyl-induced respiratory depression following the 50 μg/kg fentanyl dose and shifted the % SaO_2 dose-response curve rightward (Fig. 4E,

vaccination, $F(1,14) = 17.7$, $p < 0.001$; interaction, $F(5,70) = 9.1$, $p < 0.001$; fentanyl dose, $F(2,28.1) = 49.7$, $p < 0.001$). Fentanyl significantly decreased % SaO_2 following 25 μg/kg in sKLH vaccinated rats, but only after 100 μg/kg in the F-sKLH group, compared to their baseline values. Naloxone completely reversed fentanyl-induced % SaO_2 in the F-sKLH vaccinated group, but not in controls ($p < 0.05$). There was no effect of F-sKLH on fentanyl-induced bradycardia (Fig. 4F, vaccination, $F(1,14) = 2.09$, $p = 0.17$; interaction, $F(5,70) = 3.25$, $p < 0.05$; fentanyl dose, $F(1.65,23.0) = 4.5$, $p < 0.05$). However, fentanyl significantly decreased the heart rate in sKLH, but not in F-sKLH, treated rats compared to their baseline ($p < 0.05$). Naloxone completely reversed fentanyl-induced bradycardia in both groups.

Serum fentanyl concentrations were significantly higher in F-sKLH vaccinated rats compared to controls ($p < 0.001$) following the 100 μg/kg cumulative s.c. fentanyl dose (Fig. 5A). Brain fentanyl concentrations were 73% lower in F-sKLH vaccinated rats compared to controls following the 100 μg/kg cumulative s.c. fentanyl dose (Fig. 5B, $p < 0.01$).

Discussion

This study found that: 1) F-sKLH attenuated fentanyl-induced respiratory depression and antinociception in rats; 2) F-KLH selectively reduced the antinociceptive effects of fentanyl, but not of equianalgesic doses of heroin or oxycodone *in vivo; 3)* F-sKLH preserved naloxone's reversal of fentanyl-induced effects; and 4) F-KLH and F-sKLH reduced brain fentanyl levels following administration of large fentanyl doses. These data demonstrate that a fentanyl vaccine can effectively reduce fentanyl's effects, including its respiratory depressive effects, when formulated either on the native KLH or its GMP-grade version sKLH, which were both formulated in FDA-approved alum adjuvant and delivered i.m., the most common route of immunization for vaccines.

Fentanyl-induced overdose is characterized by marked respiratory depression, leading to death if respiration is not restored either through reversal (naloxone) or ventilation and oxygenation (Boyer, 2012). Fentanyl-induced respiratory depression may occur at different doses in humans than in rats. In the current study, fentanyl induced respiratory depression at s.c. cumulative fentanyl doses above 12.5 – 25 μg/kg in sKLH treated and naïve rats. In humans, sublingual doses of 800 μg (11 μg/kg in a 70 kg human) caused respiratory depression after 2 hours in all 12 subjects (Lister et al., 2011). In another study, apnea was reported in human subjects at an i.v. fentanyl dose as low as 2.9 μg/kg, and that prolonged apnea occurred at 7.1 μg/kg, leading the investigators to halt using this dose for the remainder of the study (Dahan et al., 2005). In this same study, respiratory depression measured in rats was reported in the range of 50 – 90 μg/kg i.v., and although these doses were infused over a period of 20 minutes to avoid death, suggesting a 10 times higher potency to induce respiratory depression in humans compared to rats.

In this study, F-sKLH attenuated fentanyl-induced respiratory depression up to a cumulative s.c. fentanyl dose of 50 μg/kg (4 times higher than in sKLH group), suggesting that fentanyl vaccines can block fentanyl-induced respiratory depression at doses considerably larger than respiratory-depressive doses in human. Another fentanyl vaccine has been shown to reduce the respiratory depressive effects of fentanyl in dogs following an i.v. dose of 5 μg/kg fentanyl (Torten et al., 1975). However, the dogs in this study were passively immunized and the antibody concentration was not specified. It has not yet been established how effective F-sKLH would be in limiting respiratory depression following i.v. fentanyl doses. The difference seen in vaccine efficacy between these two studies may be due to differences in fentanyl pharmacokinetics in these species, vaccine formulations, or route of fentanyl administration. Nevertheless, these data suggest that fentanyl vaccines can block fentanyl's respiratory-depressive effects following various routes of administration.

Hotplate antinociception, a surrogate for addiction-related behaviors because it is mediated in the central nervous system by opioid receptors (Le Bars et al., 2001), was also reduced by vaccination with F-KLH and F-sKLH. F-KLH reduced fentanyl-induced antinociception by 60% in mice given 0.05 mg/kg fentanyl s.c. and 90% in rats given 0.035 mg/kg fentanyl s.c. In *Experiment 4,* the protective effects of F-sKLH on the hotplate antinociceptive assay extended up until a 100 μg/kg fentanyl s.c. dose (a 5.4-fold shift compared to KLH controls). Similar findings have been reported in two previous studies. In one study, a fentanyl vaccine was able to prevent fentanyl's antinociceptive effect 90 seconds following an i.v. fentanyl dose of 100 μg/kg in mice (Torten et al., 1975). In another study, a fentanyl vaccine was able to shift the hotplate dose-response curve ED_{50} by 24-fold following cumulative s.c. doses of up to 1 mg/kg fentanyl in mice (Bremer et al., 2016).

F-KLH blocked the analgesic activity of fentanyl, but not equianalgesic doses of heroin or oxycodone. The antinociceptive potencies (ED_{50}) of fentanyl, heroin, and oxycodone (0.06, 0.62, and 1.53 mg/kg, respectively) are significantly different (Peckham and Traynor, 2006) and much larger heroin and oxycodone doses are required to achieve antinociception equivalent to that of fentanyl. *In vitro* selectivity of antibodies elicited by the fentanyl vaccine was not measured in the current study, but due to the high selectivity of antibodies towards their targeted compound and hapten for other similarly designed opioid vaccines (Pravetoni et al., 2012b; Raleigh et al., 2013; Raleigh et al., 2014; Raleigh et al., 2017), cross-reactivity towards heroin and oxycodone is unexpected. These data suggest that a fentanyl vaccine would likely block clinically relevant doses of fentanyl, but not heroin or oxycodone.

Naloxone is important for reversing fentanyl-induced respiratory depression and overdose (Rzasa Lynn and Galinkin, 2018). Ensuring its effects are maintained is critical when establishing the usefulness of opioid vaccines in humans, especially considering naloxone may need to be administered more than once due to fentanyl's high potency (Clarke et al., 2005; Boyer, 2012; Frank and Pollack, 2017; Tomassoni et al., 2017). To this end, it is noteworthy that vaccination with F-KLH in the current study did not interfere with naloxone efficacy for reversing fentanyl respiratory depression.

Both F-KLH and F-sKLH reduced fentanyl distribution to brain following a large i.v. fentanyl dose and a large cumulative s.c. fentanyl dose, respectively, despite molar ratio excesses of fentanyl dose to estimated antibody binding sites by at least 2.5. The i.v. dose given to rats in the current study was approximately 7 times higher than the i.v. dose that causes severe respiratory depression in humans (Dahan et al., 2005). Reduction of brain fentanyl has been reported by another group using one fentanyl vaccine following a 0.2 mg/kg s.c. fentanyl dose (Bremer et al., 2016), but this effect was not replicated in another study by the same group using a different

fentanyl vaccine following a 0.1 mg/kg i.v. fentanyl dose (Hwang et al., 2018). While there was no clear explanation for that discrepancy, differences in fentanyl vaccine potency between those two vaccines and differences in dosing route are most likely the cause. Drug dosing route has been shown to affect addiction vaccine efficacy in at least one oxycodone vaccine which showed greater reduction of brain oxyocodone concentrations following s.c. dosing (44% reduction) than following i.v. dosing (12% reduction), likely due to slower absorption following s.c. dosing compared to i.v. dosing (Raleigh et al., 2018). This route effect could have contributed to the large (90%) decrease in brain fentanyl levels with vaccination in the current study when fentanyl was administered s.c.

The doses of fentanyl used in the current study generated clinically-relevant serum fentanyl concentrations in the range of 5 – 30 ng/mL. In humans, therapeutic serum concentrations of fentanyl show a C_{max} ranging from 0.2 – 0.9 ng/mL following sublingual, intranasal, transmucosal fentanyl, or i.v. administration of fentanyl (Nave et al., 2013; Parikh et al., 2013), while unintentional overdose of transdermal patches show fentanyl blood concentrations ranging from 5 – 28 ng/mL (Jumbelic, 2010) and respiratory depression at plasma concentrations of 2.5 – 6.3 ng/mL in humans (Mildh et al., 2001).

One limitation is that control rats in *Experiment 2* had an unexpectedly low % MPE of 41%. This low % MPE may be due to fentanyl's small therapeutic window and small deviations in the fentanyl dose given to rats may have greatly affected hotplate antinociception results in the current study. Nevertheless, F-KLH significantly reduced fentanyl-induced antinociception.

Fentanyl remains the most common fentanyl-like adulterant in counterfeit pills and most commonly abused fentanyl-like opioid and the use of fentanyl analogs changes rapidly with the emergence of new analogs and their availability (O'Donnell et al., 2017; Armenian et al., 2018).

The current data suggests that F-sKLH could potentially be used as a prophylactic to reduce the side effects of fentanyl, alone or in conjunction with naloxone, and as a potential therapeutic for fentanyl abuse in humans.

JPET Fast Forward. Published on November 8, 2018 as DOI: 10.1124/jpet.118.253674
This article has not been copyedited and formatted. The final version may differ from this version.

Acknowledgements

The authors thank Danielle Burroughs for technical support.

Authorship Contributions

Participated in research design: Raleigh, Le Naour, Pentel, Pravetoni

Conducted experiments: Raleigh, Baruffaldi, Peterson, Le Naour

Contributed new reagents or analytical tools: Baruffaldi, Le Naour, Harmon, Vigliaturo, Pravetoni

Performed data analysis: Raleigh, Peterson, Le Naour, Pentel, Pravetoni

Wrote or contributed to the writing of the manuscript: Raleigh, Le Naour, Pentel, Pravetoni

References

Armenian P, Vo KT, Barr-Walker J and Lynch KL (2018) Fentanyl, fentanyl analogs and novel synthetic opioids: A comprehensive review. *Neuropharmacology* **134**:121-132.

Bazin-Redureau MI, Renard CB and Scherrmann JM (1997) Pharmacokinetics of heterologous and homologous immunoglobulin G, F(ab')2 and Fab after intravenous administration in the rat. *The Journal of pharmacy and pharmacology* **49**:277-281.

Boyer EW (2012) Management of opioid analgesic overdose. *The New England journal of medicine* **367**:146-155.

Bremer PT and Janda KD (2012) Investigating the effects of a hydrolytically stable hapten and a Th1 adjuvant on heroin vaccine performance. *J Med Chem* **55**:10776-10780.

Bremer PT, Kimishima A, Schlosburg JE, Zhou B, Collins KC and Janda KD (2016) Combatting Synthetic Designer Opioids: A Conjugate Vaccine Ablates Lethal Doses of Fentanyl Class Drugs. *Angew Chem Int Ed Engl* **55**:3772-3775.

Bremer PT, Schlosburg JE, Banks ML, Steele FF, Zhou B, Poklis JL and Janda KD (2017) Development of a Clinically Viable Heroin Vaccine. *Journal of the American Chemical Society* **139**:8601-8611.

Bremer PT, Schlosburg JE, Lively JM and Janda KD (2014) Injection route and TLR9 agonist addition significantly impact heroin vaccine efficacy. *Molecular pharmaceutics* **11**:1075-1080.

Clarke SF, Dargan PI and Jones AL (2005) Naloxone in opioid poisoning: walking the tightrope. *Emergency medicine journal : EMJ* **22**:612-616.

Dahan A, Yassen A, Bijl H, Romberg R, Sarton E, Teppema L, Olofsen E and Danhof M (2005) Comparison of the respiratory effects of intravenous buprenorphine and fentanyl in humans and rats. *British journal of anaesthesia* **94**:825-834.

DEA (2016a) Counterfeit prescription pills containing fentanyls: A global threat, in *DEA Intelligence Brief* (Agency DE ed) p 9.

DEA (2016b) National Drug Threat Assessment: Summary, in p 182.

Evans LE, Swainson CP, Roscoe P and Prescott LF (1973) Treatment of drug overdosage with naloxone, a specific narcotic antagonist. *Lancet* **1**:452-455.

Frank RG and Pollack HA (2017) Addressing the Fentanyl Threat to Public Health. *The New England journal of medicine* **376**:605-607.

Henderson GL, Frincke J, Leung CY, Torten M and Benjamini E (1975) Antibodies to fentanyl. *The Journal of pharmacology and experimental therapeutics* **192**:489-496.

Hug CC, Jr. and Murphy MR (1981) Tissue redistribution of fentanyl and termination of its effects in rats. *Anesthesiology* **55**:369-375.

Huynh NH, Tyrefors N, Ekman L and Johansson M (2005) Determination of fentanyl in human plasma and fentanyl and norfentanyl in human urine using LC-MS/MS. *J Pharm Biomed Anal* **37**:1095-1100.

Hwang CS, Smith LC, Natori Y, Ellis B, Zhou B and Janda KD (2018) Efficacious Vaccine against Heroin Contaminated with Fentanyl. *ACS Chem Neurosci* **9**:1269-1275.

Jones CM, Einstein EB and Compton WM (2018) Changes in Synthetic Opioid Involvement in Drug Overdose Deaths in the United States, 2010-2016. *JAMA : the journal of the American Medical Association* **319**:1819-1821.

Jumbelic MI (2010) Deaths with transdermal fentanyl patches. *Am J Forensic Med Pathol* **31**:18-21.

Langham S, Wright A, Kenworthy J, Grieve R and Dunlop WCN (2018) Cost-Effectiveness of Take-Home Naloxone for the Prevention of Overdose Fatalities among Heroin Users in the United Kingdom. *Value Health* **21**:407-415.

Le Bars D, Gozariu M and Cadden SW (2001) Animal models of nociception. *Pharmacological reviews* **53**:597-652.

Lister N, Warrington S, Boyce M, Eriksson C, Tamaoka M and Kilborn J (2011) Pharmacokinetics, safety, and tolerability of ascending doses of sublingual fentanyl, with and without naltrexone, in Japanese subjects. *J Clin Pharmacol* **51**:1195-1204.

Matyas GR, Mayorov AV, Rice KC, Jacobson AE, Cheng K, Iyer MR, Li F, Beck Z, Janda KD and Alving CR (2013) Liposomes containing monophosphoryl lipid A: a potent adjuvant system for inducing antibodies to heroin hapten analogs. *Vaccine* **31**:2804-2810.

Mildh LH, Scheinin H and Kirvela OA (2001) The concentration-effect relationship of the respiratory depressant effects of alfentanil and fentanyl. *Anesthesia and analgesia* **93**:939-946.

Molina-Martinez LM, Gonzalez-Espinosa C and Cruz SL (2014) Dissociation of immunosuppressive and nociceptive effects of fentanyl, but not morphine, after repeated administration in mice: fentanyl-induced sensitization to LPS. *Brain Behav Immun* **42**:60-64.

Nave R, Schmitt H and Popper L (2013) Faster absorption and higher systemic bioavailability of intranasal fentanyl spray compared to oral transmucosal fentanyl citrate in healthy subjects. *Drug Deliv* **20**:216-223.

O'Donnell JK, Halpin J, Mattson CL, Goldberger BA and Gladden RM (2017) Deaths Involving Fentanyl, Fentanyl Analogs, and U-47700 - 10 States, July-December 2016. *MMWR Morb Mortal Wkly Rep* **66**:1197-1202.

Parikh N, Goskonda V, Chavan A and Dillaha L (2013) Single-dose pharmacokinetics of fentanyl sublingual spray and oral transmucosal fentanyl citrate in healthy volunteers: a randomized crossover study. *Clin Ther* **35**:236-243.

Peckham EM and Traynor JR (2006) Comparison of the antinociceptive response to morphine and morphine-like compounds in male and female Sprague-Dawley rats. *The Journal of pharmacology and experimental therapeutics* **316**:1195-1201.

Pravetoni M, Le Naour M, Harmon TM, Tucker AM, Portoghese PS and Pentel PR (2012a) An oxycodone conjugate vaccine elicits drug-specific antibodies that reduce oxycodone distribution to brain and hot-plate analgesia. *The Journal of pharmacology and experimental therapeutics* **341**:225-232.

Pravetoni M, Le Naour M, Tucker AM, Harmon TM, Hawley TM, Portoghese PS and Pentel PR (2013) Reduced antinociception of opioids in rats and mice by vaccination with immunogens containing oxycodone and hydrocodone haptens. *J Med Chem* **56**:915-923.

Pravetoni M, Raleigh MD, Le Naour M, Tucker AM, Harmon TM, Jones JM, Birnbaum AK, Portoghese PS and Pentel PR (2012b) Co-administration of morphine and oxycodone vaccines reduces the distribution of 6-monoacetylmorphine and oxycodone to brain in rats. *Vaccine* **30**:4617-4624.

Raleigh MD, Laudenbach M, Baruffaldi F, Peterson SJ, Roslawski MJ, Birnbaum AK, Carroll FI, Runyon SP, Winston S, Pentel PR and Pravetoni M (2018) Opioid Dose- and Route-

Dependent Efficacy of Oxycodone and Heroin Vaccines in Rats. *The Journal of pharmacology and experimental therapeutics* **365**:346-353.

Raleigh MD, Pentel PR and LeSage MG (2014) Pharmacokinetic correlates of the effects of a heroin vaccine on heroin self-administration in rats. *PloS one* **9**:e115696.

Raleigh MD, Peterson SJ, Laudenbach M, Baruffaldi F, Carroll FI, Comer SD, Navarro HA, Langston TL, Runyon SP, Winston S, Pravetoni M and Pentel PR (2017) Safety and efficacy of an oxycodone vaccine: Addressing some of the unique considerations posed by opioid abuse. *PloS one* **12**:e0184876.

Raleigh MD, Pravetoni M, Harris AC, Birnbaum AK and Pentel PR (2013) Selective effects of a morphine conjugate vaccine on heroin and metabolite distribution and heroin-induced behaviors in rats. *The Journal of pharmacology and experimental therapeutics* **344**:397-406.

Riches JR, Read RW, Black RM, Cooper NJ and Timperley CM (2012) Analysis of clothing and urine from Moscow theatre siege casualties reveals carfentanil and remifentanil use. *Journal of analytical toxicology* **36**:647-656.

Rudd RA, Seth P, David F and Scholl L (2016) Increases in Drug and Opioid-Involved Overdose Deaths - United States, 2010-2015. *MMWR Morb Mortal Wkly Rep* **65**:1445-1452.

Rzasa Lynn R and Galinkin JL (2018) Naloxone dosage for opioid reversal: current evidence and clinical implications. *Ther Adv Drug Saf* **9**:63-88.

Schlosburg JE, Vendruscolo LF, Bremer PT, Lockner JW, Wade CL, Nunes AA, Stowe GN, Edwards S, Janda KD and Koob GF (2013) Dynamic vaccine blocks relapse to compulsive intake of

heroin. *Proceedings of the National Academy of Sciences of the United States of America* **110**:9036-9041.

Schneider E and Brune K (1986) Opioid activity and distribution of fentanyl metabolites. *Naunyn Schmiedebergs Arch Pharmacol* **334**:267-274.

Seth P, Scholl L, Rudd RA and Bacon S (2018) Overdose Deaths Involving Opioids, Cocaine, and Psychostimulants - United States, 2015-2016. *MMWR Morb Mortal Wkly Rep* **67**:349-358.

Stowe GN, Vendruscolo LF, Edwards S, Schlosburg JE, Misra KK, Schulteis G, Mayorov AV, Zakhari JS, Koob GF and Janda KD (2011) A vaccine strategy that induces protective immunity against heroin. *Journal of Medicinal Chemistry* **54**:5195-5204.

Tomassoni AJ, Hawk KF, Jubanyik K, Nogee DP, Durant T, Lynch KL, Patel R, Dinh D, Ulrich A and D'Onofrio G (2017) Multiple Fentanyl Overdoses - New Haven, Connecticut, June 23, 2016. *MMWR Morb Mortal Wkly Rep* **66**:107-111.

Torten M, Miller CH, Eisele JH, Henderson GL and Benjamini E (1975) Prevention of the effects of fentanyl by immunological means. *Nature* **253**:565-566.

Wheeler E, Jones TS, Gilbert MK, Davidson PJ, Centers for Disease C and Prevention (2015) Opioid Overdose Prevention Programs Providing Naloxone to Laypersons - United States, 2014. *MMWR Morb Mortal Wkly Rep* **64**:631-635.

Wong J (2012) Naloxone and nalmefene, in *Poisoning and Drug Overdose* (K.R. O ed) pp 514-517, McGraw Hill, New York.

Footnotes

This work was supported by the National Institutes of Health National Institute on Drug Abuse [Grants DA026300, DA038876].

Legends for Figures

Figure 1. Structure of A) fentanyl and B) fentanyl-based hapten.

Figure 2. *Experiment 1;* F-KLH reduces fentanyl-induced antinociceptive effects and increases serum fentanyl concentrations in mice. Vaccination with F-KLH significantly reduced **A)** fentanyl-induced hotplate antinociception by 60% (Mean ± SEM) and **B)** increased serum fentanyl concentrations (Mean ± SD) compared to controls 30 min after a 0.05 mg/kg s.c. dose of fentanyl. Numbers above bars represent the percent difference from controls. ** $p < 0.01$, *** $p < 0.001$ compared to controls using unpaired t tests with Welsh's correction. n = 6/group.

Figure 3. *Experiment 2,* selectivity and pharmacokinetic efficacy of F-KLH in rats. A) Vaccination with F-KLH significantly reduced fentanyl-induced hotplate antinociception by 93% 30 min after a 0.035 mg/kg s.c. dose of fentanyl. **B and C)** F-KLH had no effect on heroin- or oxycodone-induced antinociception 30 min after a 1 mg/kg or 2.25 mg/kg dose of heroin or oxycodone, respectively. **D)** Serum fentanyl concentrations were significantly increased and **E)** brain fentanyl concentrations were significantly decreased compared to controls 4 min after a 1-min 0.05 mg/kg i.v. infusion of fentanyl. Numbers above bars represent the percent difference from controls. * $p < 0.05$, *** $p < 0.001$ compared to controls. Mean ± SD (D and E), Mean ± SEM (A, B, and C), n = 12/group (A, D, and E) and n = 6/group (B and C).

Figure 4. Fentanyl dose-response and F-sKLH effects on hotplate antinociception, respiratory depression, and bradycardia in rats. Fentanyl was administered s.c. every 15 min at increasing doses in non-immunized rats and the doses listed are the cumulative dose received. **A)** Effect of fentanyl on hotplate antinociception. Latency to respond is capped at 60 seconds. Naloxone (0.1 mg/kg, s.c.) was administered 15 min after the final fentanyl dose. **B)** Effect of fentanyl on respiratory depression measured as SaO_2. **C)** Effect of fentanyl on heart rate. ** p <

0.01, *** $p < 0.001$ for the difference between values compared to baseline. **D)** Vaccine effects on fentanyl-induced antinociception. **E)** Vaccine effects on fentanyl-induced respiratory depression measured as SaO_2. **F)** Vaccine effects on fentanyl-induced decreases in heart rate. * $p < 0.05$, ** $p < 0.01$, *** $p < 0.001$ for differences from baseline within groups. # $p < 0.05$, ## $p < 0.01$, and ### $p < 0.001$ for the difference between groups at each dose. There were no differences between groups in latency to respond, SaO_2, or heart rate following naloxone treatment. Mean ± SD; n = 8/group.

Figure 5. ***Experiment 4,*** **F-sKLH alters fentanyl distribution in serum and to the brain.** F-sKLH vaccination **A)** increases serum and **B)** decreases brain fentanyl distribution by 73% 30 minutes after receiving a cumulative 0.1 mg/kg s.c. fentanyl dose. Numbers above bars represent the percent difference from controls. Mean ± SD, $p < 0.001$ compared to controls using unpaired t tests with Welch's correction.

JPET Fast Forward. Published on November 8, 2018 as DOI: 10.1124/jpet.118.253674
This article has not been copyedited and formatted. The final version may differ from this version.

Schemes

Scheme 1. Synthetic pathway to hapten **[8]**. *Reactants* a. 2-(Boc-amino)ethylbromide , K_2CO_3, acetonitrile, 80°C , 88%; b. aniline, AcOH, $NaBH_3CN$, CH_2Cl_2, 80°C, 86%; c. propionyl chloride, DIPEA, CH_2Cl_2, rt, 95%; d. TFA/ CH_2Cl_2 (2/8-v/v), rt, quantitative; e. glutaric anhydride, pyridine, CH_2Cl_2, rt, quantitative; f. $(Gly)_4$-OtBu, HBTU, DIPEA, CH_2Cl_2, rt, 74%; TFA/ CH_2Cl_2 (2/8-v/v), rt, 92%; g. TFA/ CH_2Cl_2 (2/8-v/v), rt, 92%.

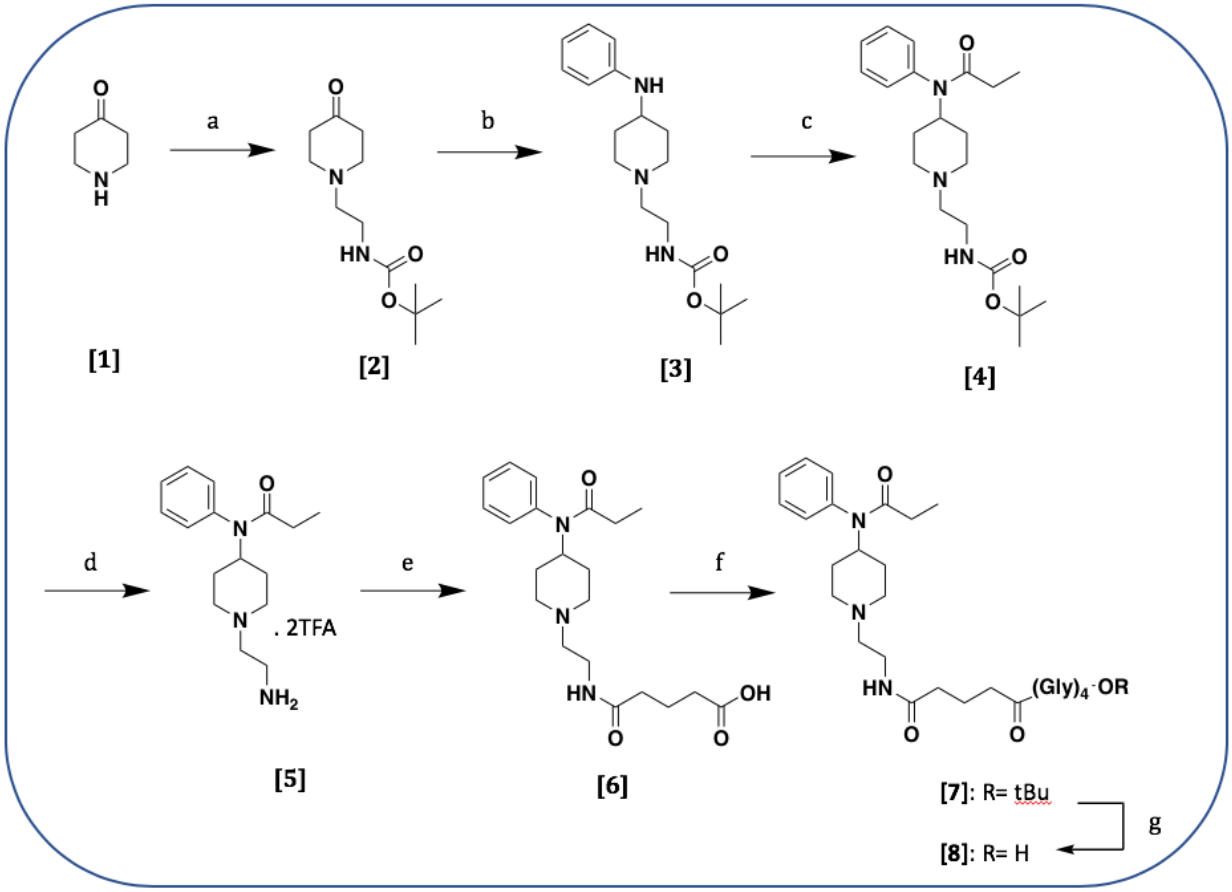

JPET Fast Forward. Published on November 8, 2018 as DOI: 10.1124/jpet.118.253674
This article has not been copyedited and formatted. The final version may differ from this version.

Figures

Figure 1

A

Fentanyl

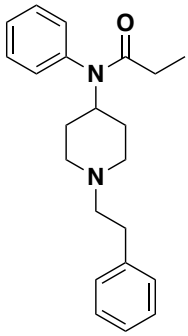

B

Fentanyl hapten

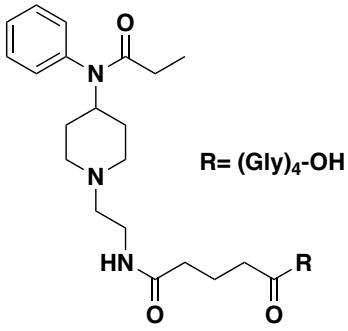

JPET Fast Forward. Published on November 8, 2018 as DOI: 10.1124/jpet.118.253674
This article has not been copyedited and formatted. The final version may differ from this version.

Figure 2

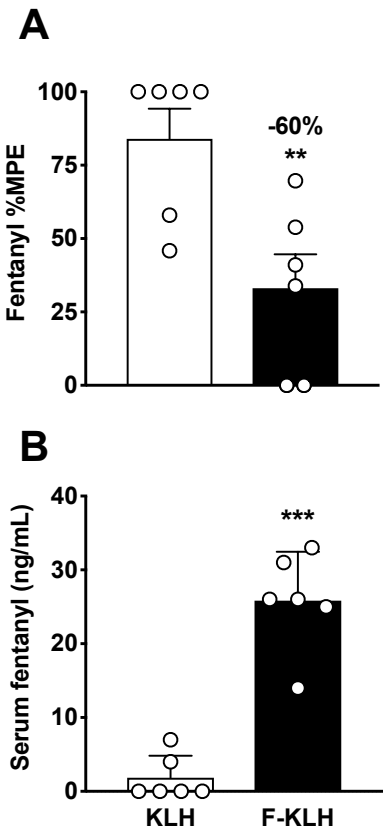

JPET Fast Forward. Published on November 8, 2018 as DOI: 10.1124/jpet.118.253674
This article has not been copyedited and formatted. The final version may differ from this version.

Figure 3

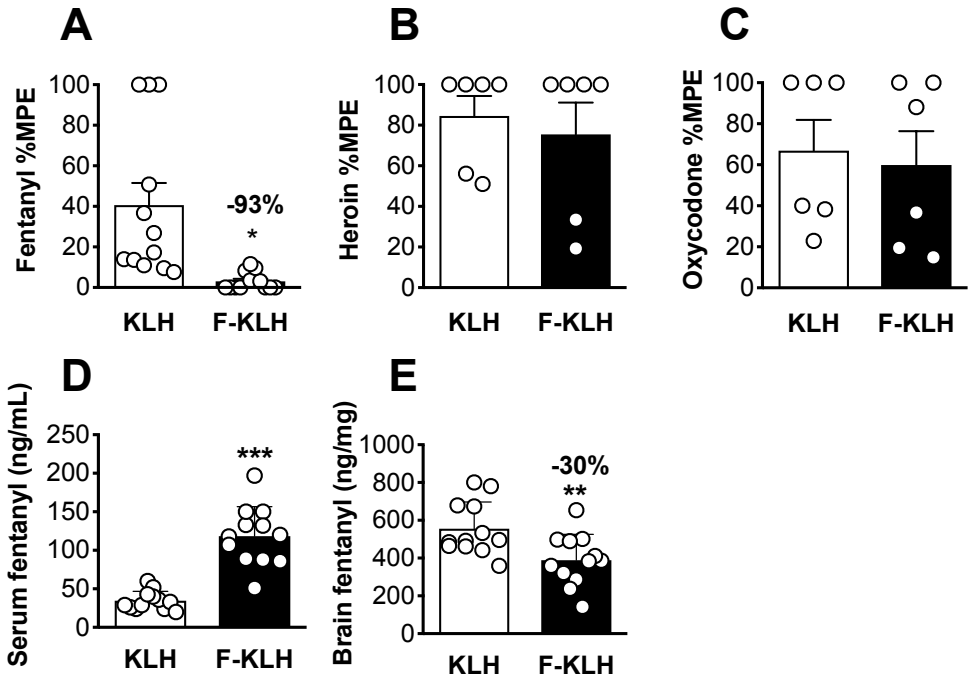

JPET Fast Forward. Published on November 8, 2018 as DOI: 10.1124/jpet.118.253674
This article has not been copyedited and formatted. The final version may differ from this version.

Figure 4

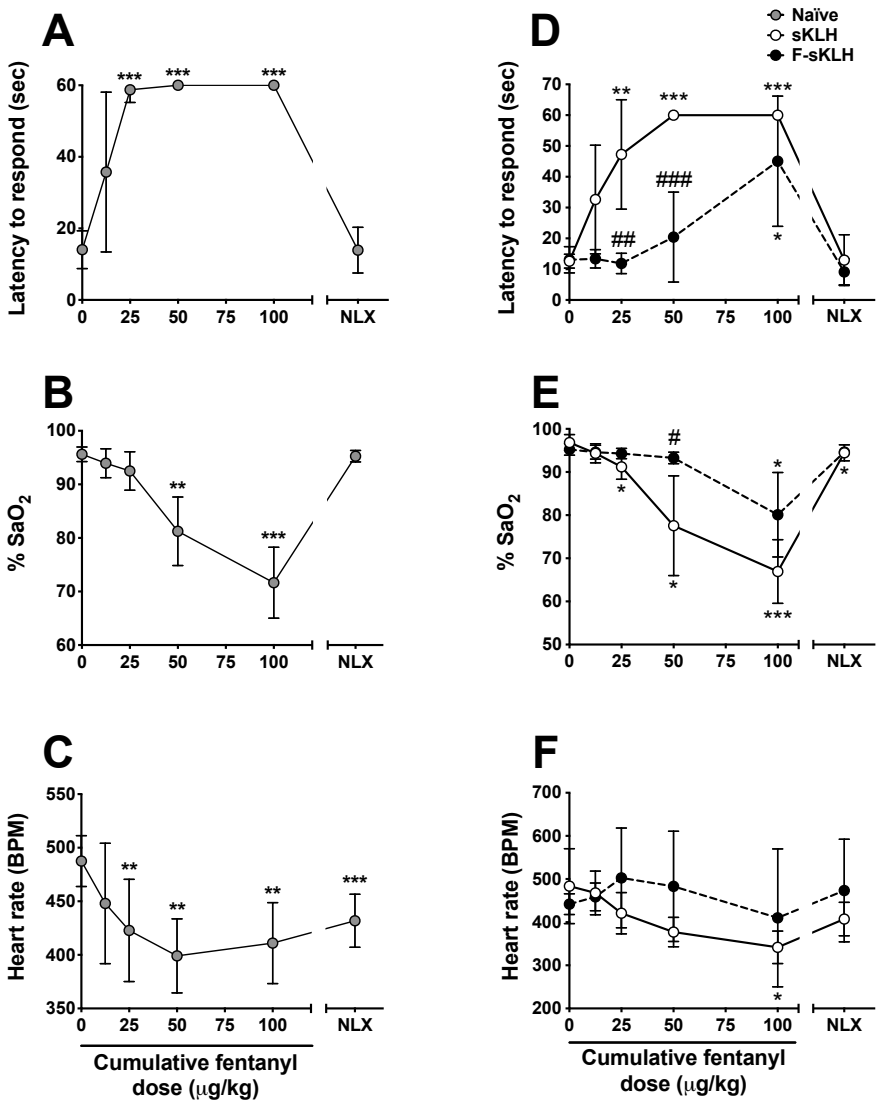

JPET Fast Forward. Published on November 8, 2018 as DOI: 10.1124/jpet.118.253674
This article has not been copyedited and formatted. The final version may differ from this version.

Figure 5